AALBORG UNIVERSITY

DENMARK

Hybrid Energy Storage Systems for Voltage Stabilization in Shipboard Microgrids

Mutarraf, Muhammad Umair; Terriche, Yacine; Nasir, Mashood; Niazi, Kamran Ali Khan; Vasquez, Juan C.; Guerrero, Josep M.

Hybrid Energy Storage Systems for Voltage Stabilization in Shipboard Microgrids

Muhammad Umair Mutarraf
Department of Energy Technology
Aalborg University
Aalborg, Denmark
mmu@et.aau.dk

Yacine Terriche
Department of Energy Technology
Aalborg University
Aalborg, Denmark
yte@et.aau.dk

Mashood Nasir
Department of Energy Technology
Aalborg University
Aalborg, Denmark
mnas@et.aau.dk

Kamran Ali Khan Niazi
Department of Energy Technology
Aalborg University
Aalborg, Denmark
kkn@et.aau.dk

Juan C. Vasquez
Department of Energy Technology
Aalborg University
Aalborg, Denmark
juq@et.aau.dk

Josep M. Guerrero
Department of Energy Technology
Aalborg University
Aalborg, Denmark
joz@et.aau.dk

Abstract—Due to increasing environmental concerns associated with the fossil fuel consumption and greenhouse emissions by marine vessels, world is moving towards sustainable energy resources such as solar, wind and so on. Renewable energy sources are found out to be a significant source of energy as they are sustainable and clean as compared to traditional generation sources, for instance, the burning of fossil fuels, diesel generators, steam engines, etc. As solar energy is one of the cheapest, abundant and cleanest source of energy, therefore, it has the potential to be the most utilized source of energy along with energy storage systems (ESS) for future yachts and ferries. However, partial shading effect and intermittent nature of photovoltaic (PV) systems cause fluctuations in voltage that can potentially disturb the voltage profile, therefore may instigate instability in shipboard microgrids, if not properly managed. This paper, therefore, proposes a hybrid energy storage system (HESS) comprising of Lithium-ion (Li-ion) battery and ultra-capacitor having the capability to mitigate fluctuations caused by the partial shading effect in PV panels. The control system is based on frequency sharing approach in which high-frequency components are handled by the ultra-capacitor whereas low-frequency components are handled by the Li-ion battery. The proposed methodology is simulated using MATLAB/ SINULINK and various scenarios of power sharing are highlighted for the validation of the proposed scheme.

Index Terms—Frequency sharing, hybrid energy storage systems (HESS), shipboard microgrids, battery energy storage system (BESS), partial shading, photovoltaic (PV) systems.

I. Introduction

The cost of energy and environmental problems such as global warming are of greater importance in shipboard microgrids in recent times. The increase in emissions from marine ships have grabbed attention, which made the shipboard industry to think regarding alternative fuels and sustainable energy sources. It can be seen from Fig. 1 that CO_2 emissions from the international shipping is 2% of the global CO_2 emissions [1]. It is stated in a recent study by the European Parliament that emissions by shipping should be reduced around 13 % by 2030 and around 63 % by 2050 as compared to the 2005

level. It is observed that maritime emissions are increased by 3 % per year between 1990 and 2010, which is higher than the increase in global house gas emissions, i.e., 1.1 % [2].
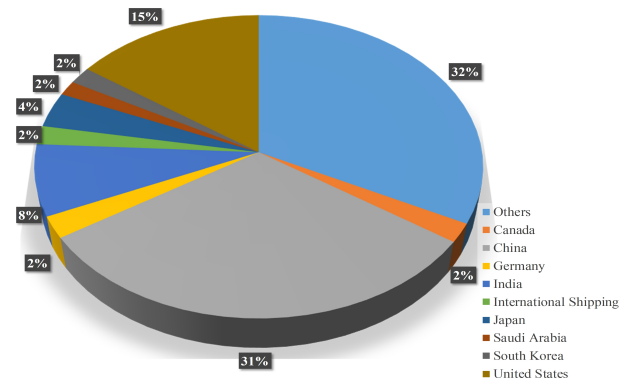

Fig. 1: Global CO_2 emissions from all over the world [1].

As of today, more than 90% of the cargo is transported by marine vessels [3] that increases the use of fossil fuel consumption and greenhouse emissions. Therefore, alternative generation sources such as solar and wind should be implemented as these sources are abundant and help to minimize the fuel consumption such that to satisfy the limitations imposed by the shipboard authorities. The use of solar panels in yachts and ferries have increased as they are abundant and cost-effective but the intermittent nature of solar panels, weather conditions and continuous movement of ship limit the use of solar panels on ships. Further, the partial shading effect that is caused by the higher deck, obstacles or by the shading of clouds causes the hot-spot problem that results into efficiency and safety problems of PV panels [4].

The study in [5] integrated flywheel energy storage system (FESS) with the PV systems to improve the power quality and smooth the fluctuations on an oil tanker. FESS is capable to mitigate the short-term deviations (seconds to minutes) only,

however, for long-term deviations author did not consider any high energy density device in their proposed approach. K. J. Lee et al [6] used PV, Diesel generator (DG), and battery energy storage system (BESS) to minimize the consumption of fuel. Optimal sizing of HESS comprising of lead-acid battery, Li-ion battery, and ultra-capacitor proposed in [7] to mitigate the fluctuations caused the PV systems such that slow power deviations are catered by the lead-acid and Li-ion battery whereas fast power deviations are catered by the ultra-capacitor. Although, a HESS system is used to mitigate the short-term and long-term fluctuations but in their proposed approach they did not consider the partial shading effect. K. Bellache et al. [8] used an energy management system based on the frequency sharing approach for an electric boat. The load profile is shared in such a way that high-frequency components are allocated to Li-ion battery and low-frequency components are allocated to the diesel generator such that to minimize the effect of fluctuations on DG in order to increase the lifetime and performance of DG. However, their approach adds burden on generator by allocating low-frequency penetrations, moreover, their approach can decrease the life-time of the battery as well. The model predictive control (MPC) based strategy is proposed in [9] such that to regulate the dc-link voltage and control the generation of DG of the integrated power system (IPS). IPS in this study comprises of fuel cell (FC), BESS, and DG. A. Dolatabadi et al. [10] proposes stochastic programming methodology to optimize the size of a hybrid ship with ESS, PV, and DG. However, the aforementioned studies didn't take in count the partial shading effect of PV panels.

This paper, therefore, proposes a HESS system comprising of ultra-capacitor and Li-ion battery for DC shipboard microgrids to stabilize the dc-link voltage that is caused by the partial shading effect and intermittent nature of PV panels. The proposed system and the control methodology has the capability to provide an instant compensation based upon the frequency sharing, therefore provides constant voltage and avoid system instability etc. The frequency sharing approach based on proportional-integral (PI) control using low pass filter is utilized in this study such that high-frequency deviations are catered by the ultra-capacitor and the low-frequency deviations are smoothed by the Li-ion battery. Further, electric propulsion is used in this study and the use of DC microgrids improves the efficiency of the whole system [11]– [12].

The rest of this paper is organized as follows. In section II, a comparison of several ESS is conducted. The mathematical modeling of PV, battery, and ultra-capacitor is presented in Section III. Section IV presents the control strategy of a hybrid PV/battery/Ultra-capacitor. The simulation results are presented in Section V to validate the proposed approach. Finally, the conclusion drawn from this study is presented in Section VI.

II. ENERGY STORAGE TECHNOLOGIES

In recent times, lead-acid batteries are used in only those applications such as Uninterruptible Power Supplies (UPS)

where cost is a major concern. However, the lower energy density and a short cycle life of this type of ESS limit its use for shipboard microgrid application. Among other types of batteries, Li-ion battery is considered as the best suitable candidate for shipboard microgrids. As, Li-ion based batteries exhibit a quite high round-trip efficiency, very low self-discharge, and low maintenance as well. The only hindrance in its use is the higher cost. Due to their low power density, batteries are only suitable for applications where high energy density is required. On the other hand, the applications, which require high power for a short duration of time, ultra-capacitor and flywheel can be utilized. The ultra-capacitor is utilized in this study due to its higher power density as compared to the flywheel [13]– [14]. Table I refers to the technical features of several types of ESS. The ultra-capacitor can be hybridized with battery in two manners either it can be internally hybridized such as ultra-battery or externally hybridized. As, internal hybridization at this stage is not a mature technology, therefore, in this study, hybridization is done by a hard-wired connection between Li-ion battery and ultra-capacitor.

TABLE I: Comparison of different ESS devises [13]– [14].

ESS	Efficiency	Energy Density	Power Density	Life Time
	(%)	(kWh/kg)	(kW/kg)	(years)
Ultra-Capacitor	85–98	20+	100,000+	10–20
Flywheel	90–95	10–30	400–1500	20–30
Lead Acid	65–80	30–50	75–300	3–12
Li-ion	90–97	75–200	150–315	5–15

III. MODEL OF DC SHIPBOARD MICROGRIDS

The proposed model used in this study is shown in Fig. 2 that consists of PV array, BESS, ultra-capacitor. BESS and Ultra-capacitor energy storage system (UCESS) are integrated in parallel to the dc-link by using a buck-boost converter to stabilize the voltage and enhance the reliability and stability of the shipboard microgrid. Many devices and energy sources such as batteries, PV panels, and fuel cells operate on DC, hence the less use of power electronics might improve efficiency. Further, the DC power system has an advantage of a lack of reactive power that causes line losses and oversizing of inverters. High penetration of non-linear loads in shipboard microgrids causes instability, therefore, DC microgrid is suitable and is preferred over AC microgrid. Hence, DC-microgrid is employed in this paper due to its higher reliability, efficiency, and stability. The steady state power flow in the proposed model is illustrated in equation 1.

$$P_t = P_{PV} + P_{BESS} + P_{UCESS} - P_{Load} \qquad (1)$$

where P_t is the total power of the generation sources and load, P_{PV} is power from the PV array, P_{load} shows the power of the load, P_{BESS}, and P_{UCESS} shows the power of battery and ultra-capacitor respectively.

The detailed parameters of the PV system, ultra-capacitor, and Li-ion battery utilized in this paper are given in Table II.
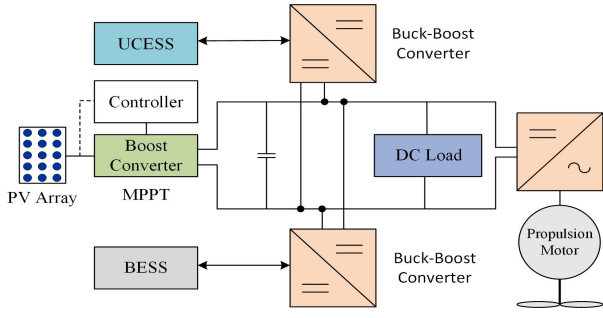
Fig. 2: Block diagram of hybrid PV/battery/UC greener ship.

TABLE II: Parameters of system components.

PV Array (SunPower SPR-305E)	Module 1 Module 2	N_s = 3, N_p = 10, I_r=1000 W/m^2 N_s = 3, N_p = 10, I_r=1000, 900, 700, and 500 W/m^2 Rated power = 305.226 W Cells per module = 96 V_{mp} = 54.7 V, I_{mp}=5.58 A
BESS (Panasonic CGR18650AF)	Rated Capacity Rated Voltage Cells	48 kWh 288 V N_s = 87, N_p = 82
UCESS (PC 2500)	Rated Capacity Rated Voltage Cells	2716 F 400 V N_s= 160, N_p=1
Load	DC Load Propulsion Motor	5 kW, 400V 10 kW, 400V

A. Modeling of PV panels

In this study, the PV panel from the Simulink library is utilized. The multi-string topology is shown in Fig. 3 is applied in this study, as this topology has an effective MPPT control, blocking diodes are not mandatory, same power generation capability as of centralized technology, and improves conversion efficiency. The Incremental conductance-based MPPT algorithm is exploited because it is considered more efficient as compared to Perturb and observe (P & O). The mathematical model of a PV array can be expressed by the equations 2-7 [15].
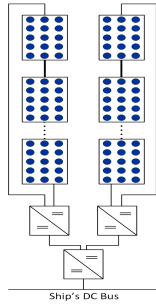

Fig. 3: Multi-string topology.

$$I_{pv} = [K_i(T - 298) + I_{sc}]\frac{I_r}{100} \quad (2)$$

where K_i is short circuit current of the cell, I_{sc} is the short circuit current (A), I_r is incident solar irradiance (W/m^2), and I_{pv} is the PV current at the 25 °C and 1000 W/m^2.

$$I_{rs} = \frac{I_{sc}}{exp(qVoc/N_s knT) - 1} \quad (3)$$

where q is charge of an electron, N_s is number of cells in series, V_{oc} is open circuit voltage (V), k is Boltzmann's constant, n is the ideality factor of diode, and I_{rs} is reverse saturation current.

$$I_o = I_{rs}[\frac{T}{T_r}]^3 exp[\frac{qE_{go}}{nk}(\frac{1}{T} - \frac{1}{T_r})] \quad (4)$$

where I_o is the saturation current, E_{go} is band gap energy of a semiconductor, and T_r is the nominal temperature.

$$V^t = \frac{kT}{q} \quad (5)$$

where V^t is thermal voltage of a diode.

$$I_{sh} = \frac{N_p/N_s V + IR_s}{R_{sh}} \quad (6)$$

where R_{sh} is the shunt resistance, N_s and N_p are number of modules connected in series and parallel respectively.

$$I = I_{ph}N_p - N_p I_o[exp(\frac{V/N_s + IR_s/N_p}{nV^t} - 1] - I_{sh} \quad (7)$$

where I is the output current.

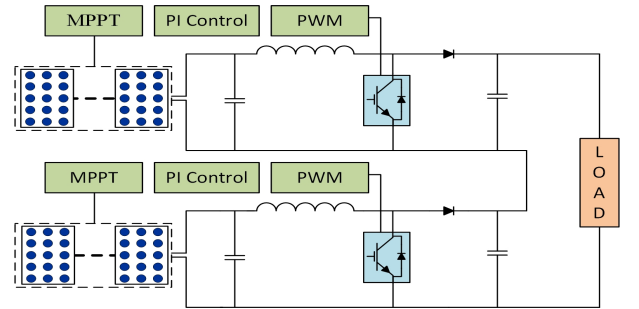The schematic diagram of the PV system with MPPT and boost converter is depicted in Fig. 4.

Fig. 4: Schematic diagram of PV systems.

Two strings of PV panels, each having three panels in series and ten in parallel is utilized in this study. The power extraction from PV can be controlled and the system has the capability to be operated in both MPPT mode as well current control mode based upon the various system parameters and the control system, which is illustrated in the next section. The side view of the ship with PV panels is illustrated in Fig. 5 whereas shading of the obstacles and clouds on the ship as illustrated in Fig. 6 adds partial shading effect which ultimately lowers the power generation capacity.
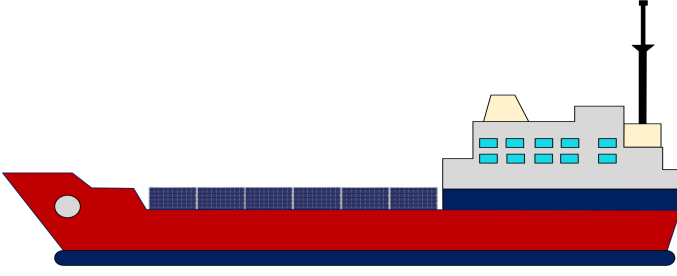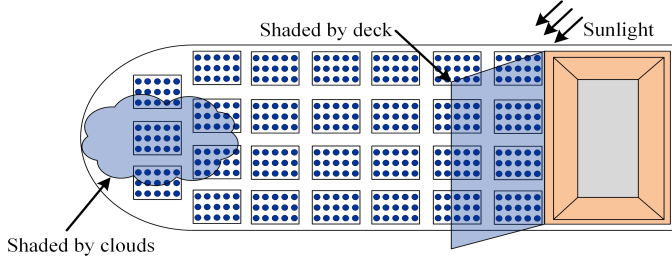
Fig. 5: Side view of the Ship.

Fig. 6: Partial shading effect on the Ship (top view).

B. Modeling of Battery

The battery models are usually categorized as an electro-chemical model and electric circuit model, the rest of the models are mainly driven from these models. The mathematical model of charging and discharging of Li-ion battery is shown in equation 8–9 respectively [15]. A mathematical model is used in this study due to the availability of cost-effective tools such as MATLAB/SIMULINK [16].

1) Charge model: For Li-ion battery the charging model is depicted in the following equation:

$$f_1(i_t, i_l, i) = E_o - K\frac{Q}{Q - i_t}i_t - K\frac{Q}{0.1Q + i_t}i_l + Aexp(-Bi_t) \tag{8}$$

2) Discharge model: For Li-ion battery the discharging model is depicted in the following equation:

$$f_2(i_t, i_l, i) = E_o - K\frac{Q}{Q - i_t}i_t - K\frac{Q}{Q - i_t}i_l + Aexp(-Bi_t) \tag{9}$$

where E_0 is constant voltage, K is the polarization constant, Q is maximum capacity of the battery, A is the exponential voltage, B is exponential capacity, i_t is the extracted capacity, i_l is low-frequency dynamics, and i is the current of battery.

C. Modeling of Ultra-capacitor

The output voltage of an ultra-capacitor can be illustrated in terms of the Stern equation [17]:

$$V_{UCESS} = \frac{Q_T N_s d}{A_i N_p \varepsilon\varepsilon_o N_e} + \frac{2RTN_e N_s}{F}sinh^{-1}$$
$$\frac{Q_T}{N_p N_e^2 A_i \sqrt{8cTR\varepsilon\varepsilon_o}} - R_{UCESS}i_{UCESS} \tag{10}$$

where V_{UCESS} is the voltage of ultra-capacitor, Q_{T} is electric charge, N_{s} and N_{p} are the number of series and parallel ultra-capacitors respectively, A_{i} is interfacial area between the electrode and electrolyte, R_{UCESS} is total resistance, R_{UCESS} is total resistance, ε is permittivity of material, d is the molecular radius, is the operating temperature, F is Faraday constant, c is molar concentration, R is ideal gas constant, and i_{UCESS} is the ultra-capacitor current.

IV. FREQUENCY SHARING CONTROL

In order to mitigate the fluctuations caused by the intermittent nature PV panels and partial shading effect, Li-ion battery is externally hybridized with ultra-capacitor. The frequency sharing control strategy is utilized in such a way that the the load current is shared between high-frequency and low-frequency components. The low-frequency deviations are catered by Li-ion battery whereas high-frequency fluctuations is smoothed by the ultra-capacitor as depicted in Fig. 7. The dc-link voltage (V_{dc}) is compared with the reference voltage, i.e., 400 and the error is then fed to the outer loop voltage controller. The low-pass filter categorize the penetrations into low and high frequency components. The lower frequency deviations are then fed to inner loop current controller and is compared with the current of battery. The error is then fed to PI controller and the PWM singal is passed onto DC-DC bi-directional converter. Similarly, the high frequency deviations is fed into inner loop current controller and is compared with ultra-capacitor current. The error is removed by a PI controller and switching signal is then fed to dc-dc bi-directional converter.
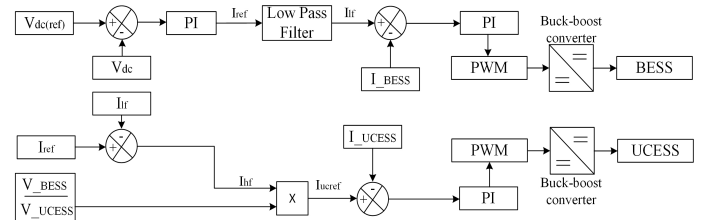

Fig. 7: Proposed Control strategy.

V. SIMULATION RESULTS

The hybrid model consisting of PV, BESS, and UCESS depicted in Fig. 2 is utilized in this paper to validate the proposed approach. The multi-string topology is adopted in this study that consists of two strings of PV panels with a number of series and parallel panels to illustrate the dynamic behavior of the system. In order to show the partial shading effect, irradiance on one of the string is kept to be constant, i.e., 1000 W/m^2. On the other hand, due to obstacles, deck shading, and shading by clouds, irradiance is varied in four steps, i.e., Case A = 1000 W/m^2, Case B= 900W/m^2, Case C= 700W/m^2, and Case D = 500 W/m^2. The voltage and power of PV array with varying irradiance are illustrated in Fig. 8(a) and Fig. 8(b) respectively.
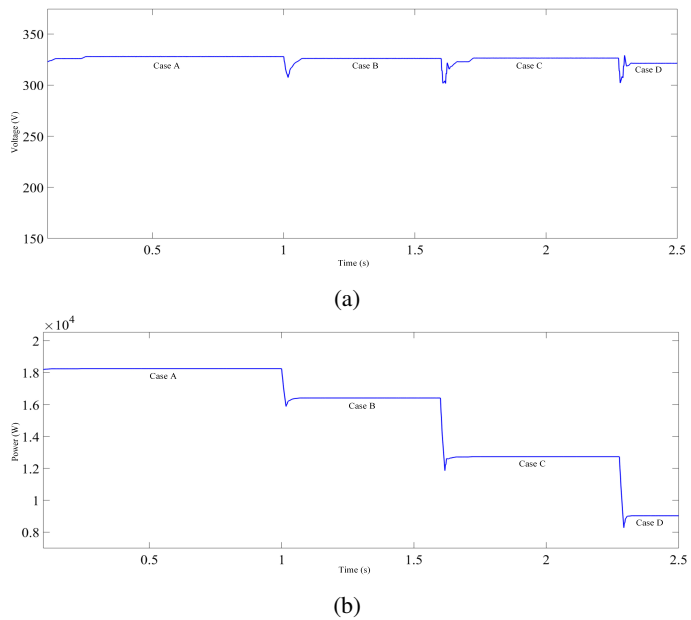
Fig. 8: Simulation results of PV array (**a**) Voltage of solar array, (**b**) Power of solar array.
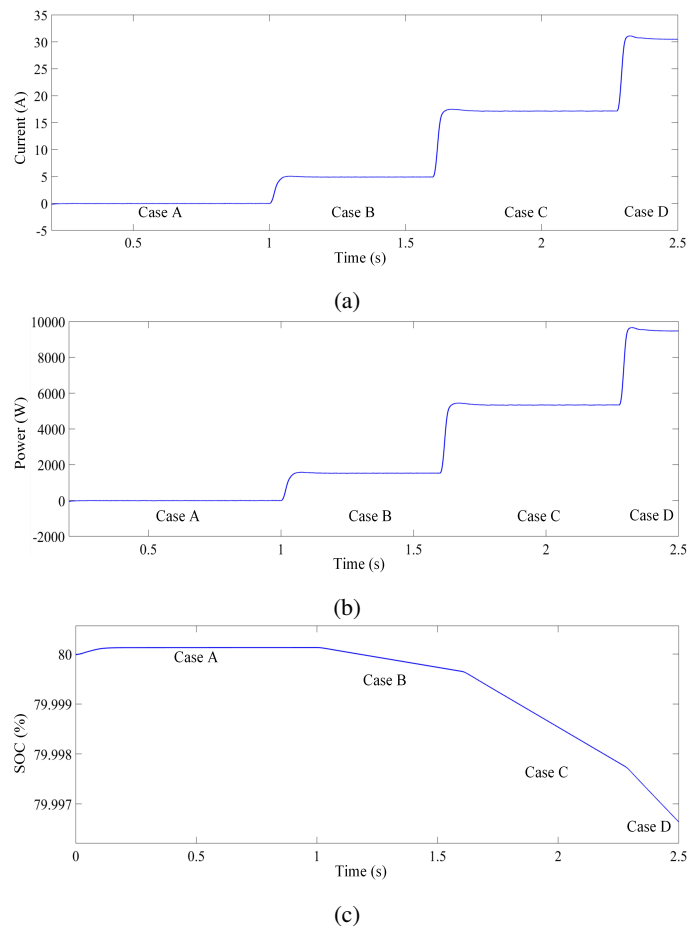

Fig. 9: Simulation results of a Li-ion battery (**a**) Current of battery, (**b**) Power of battery, (**c**) SOC of battery.

Li-ion battery is adopted in the paper to mitigate the low-frequency deviations. It can be seen from Fig. 9 (a) that till 1s battery is not contributing as during this duration PV array is generating enough power that will charge the on-board batteries as well as handle the on-board AC and DC Loads. The power of battery with varying irradiance is depicted in Fig. 9 (b). Fig. 9 (c) illustrates the state of charge (SOC) of battery. In the start, battery is getting charged as PV array is generating access power. At 1s due to variation in irradiance the battery discharges, which ultimately reduces the SOC of the battery. The UCESS is hybridized externally via hard wired connection with the battery to mitigate high-frequency fluctuations. It can be inferred from Fig. 10 (a) that at 1s, 1.6s, and 2s the high-frequency fluctuations are observed and the ultra-capacitor provides the current for a very short duration of time such that it smooth the dc-link voltage. Fig. 10 (b) refers to the power of the ultra-capacitor. Fig. 10 (c) illustrates that SOC of ultra-capacitor suddenly decreases for a very small period as soon as irradiance is varied and then remains constant. As ultra-capacitor is responsible to mitigate high-frequency fluctuations, so, the battery is responsible for rest of the period.
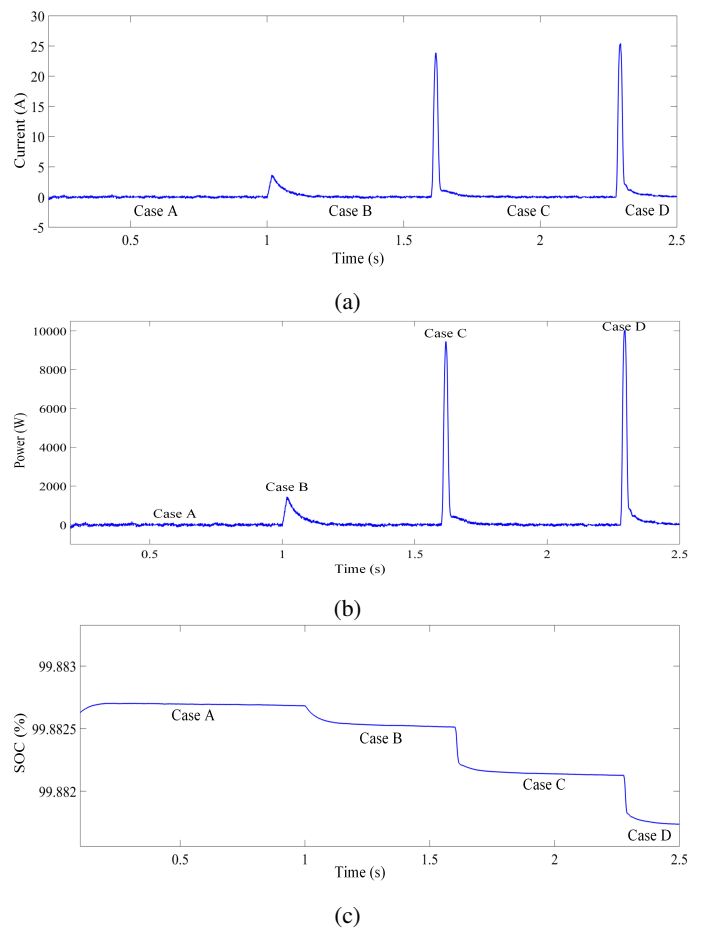

Fig. 10: Simulation results of UCESS (**a**) Current of UCESS, (**b**) Power of UCESS, (**c**) SOC of UCESS.

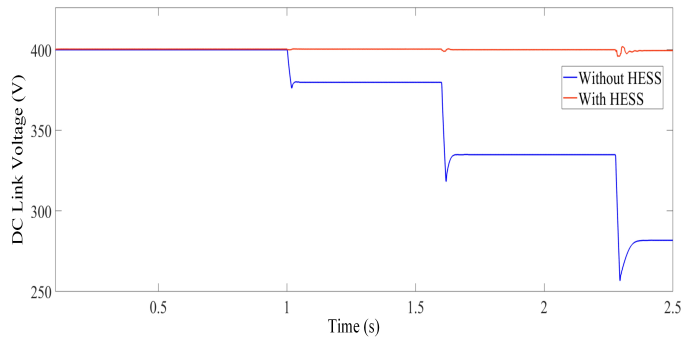The dc-link voltage fluctuates with the variation in irradi-

Fig. 11: DC Link voltage with and without HESS.

ance that occurs due to partial shading on the panels. Fig. 11 depicts the dc-link voltage with and without using HESS. It can be inferred that HESS stabilize and smooth the dc-link voltage. The comparison between integrating BESS only and HESS with the dc-link voltage to cater the fluctuations is depicted in Fig. 12. It can be seen that high-frequency fluctuations are not catered when only BESS is integrated. On the other, hand it is observed that HESS smooth both high and low-frequency deviations.
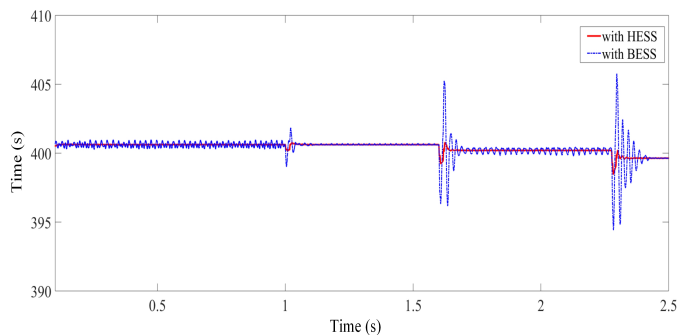

Fig. 12: DC-Link voltage with BESS and HESS.

VI. CONCLUSION

This paper presents a novel approach for smaller yachts and ferries to mitigate fluctuations that are caused by either hot-spot problem or by the intermittent nature of PV panels. In this approach, the frequency sharing approach with PI control strategy is utilized to smooth the fluctuations in such a manner that high-frequency and low-frequency deviations are shared between ultra-capacitor and Li-ion battery. Multi-string topology of PV panels is utilized in this approach such that it provides high efficiency as compared to the centralized topology. Further, the Incremental conductance-based MPPT algorithm is applied to track the maximum power point as it is considered less complex and more efficient as compared to other algorithms. The future work is based on cold-ironing of the ships that are integrated with PV arrays such that to support the nearby grid during the time when the marine vessels are at harbor.

REFERENCES

[1] G. Janssens-Maenhout, M. Crippa, D. Guizzardi, M. Muntean, E. Schaaf, J. G. J. Olivier, J. A. H. W. Peters, K. M. Schure. Fossil CO2 & GHG emissions of all world countries. *Luxembourg: Publications Office of the European Union.*, **2017**, 107877.

[2] M. Cames, J. Graichen, A. Siemens, V. Cook. Emission reduction targets for international aviation and shipping.

[3] K. Ferdows. "Keeping up with growing complexity of managing global operations. International Journal of Operations & Production Management," vol. 38, no. 2, pp.390–402, 2018.

[4] K. A. K. Niazi, Y. Yang, D. Sera. "Review of mismatch mitigation techniques for PV modules," *Iet Renewable Power Generation*, 2019.

[5] H. Lan, Y. Bai, S. Wen, D. Yu, Y. Y. Hong, J. Dai, P. Cheng. "Modeling and stability analysis of hybrid pv/diesel/ess in ship power system. *Inventions*, vol. 1, no. 1, p.5, 2016.

[6] K. J. Lee, D. Shin, D. W. Yoo, H. K. Choi, H. J. Kim. "Hybrid photovoltaic/diesel green ship operating in standalone and grid-connected mode–Experimental investigation," *Energy*, vol. 49, pp. 475–483, 2013.

[7] S. Wen, H. Lan, D. C. Yu, Q. Fu, Y. Y. Hong, L. Yu, R. Yang. "Optimal sizing of hybrid energy storage sub-systems in PV/diesel ship power system using frequency analysis," *Energy*, vol. 140, p. 198-208, 2017.

[8] K. Bellache, M. B. Camara, B. Dakyo. "Hybrid Electric Boat based on variable speed Diesel Generator and lithium-battery-using frequency approach for energy management," *Intl Aegean Conference on Electrical Machines & Power Electronics (ACEMP), 2015 Intl Conference on Optimization of Electrical & Electronic Equipment (OPTIM) & Intl Symposium on Advanced Electromechanical Motion Systems (ELEC-TROMOTION)*, pp. 744-749, 2015, IEEE.

[9] M. R. Banaei, R. Alizadeh. "Simulation-based modeling and power management of all-electric ships based on renewable energy generation using model predictive control strategy," *IEEE Intelligent Transportation Systems Magazine*, vol. 8, no. 2, p. 90–103, 2016.

[10] A. Dolatabadi, R. Ebadi, B. Mohammadi-Ivatloo. "A two-stage stochastic programming model for the optimal sizing of hybrid PV/diesel/battery in hybrid electric ship system," *Journal of Operation and Automation in Power Engineering*, vol. 7, no. 1, p. 16–26, 2019.

[11] M. Nasir, Z. Jin, H. A. Khan, N. A. Zaffar, J. C. Vasquez, J. M. Guerrero. "A decentralized control architecture applied to dc nanogrid clusters for rural electrification in developing regions," *IEEE Transactions on Power Electronics*, vol. 34, no. 2, p.1773–1785, 2018.

[12] M. Nasir, H. A. Khan, K. A. K. Niazi, Z. Jin, J. M. Guerrero, "Dualloop Control Strategy applied to PV/battery based Islanded DC microgrids for Swarm Electrification of Developing Regions," *Journal of Engineering*, 2018.

[13] M. U. Mutarraf, Y. Terriche, K. A. K. Niazi, C. L. Su, J. C. Vasquez, J. M. Guerrero. "Battery Energy Storage Systems for Mitigating Fluctuations Caused by Pulse Loads and Propulsion Motors in Shipboard Microgrids," *In 2019 IEEE 28th International Symposium on Industrial Electronics (ISIE)*, p. 1047–1052, IEEE.

[14] M. U. Mutarraf, Y. Terriche, K.A.K. Niazi, J. Vasquez, J.M. Guerrero, "Energy Storage Systems for Shipboard Microgrids–A Review," *Energies*, vol. 11, no. 12, p. 3492, 2018.

[15] Lithium-ion battery. Available Online: https://se.mathworks.com/help/physmod/sps/powersys/ref/battery.html. (accessed on 11 August 2019).

[16] P. M. Gomadam, J. W. Weidner, R. A. Dougal, R. E. White. "Mathematical modeling of lithium-ion and nickel battery systems," *Journal of power sources*, vol. 110, p. 267-284, 2002.

[17] Ultra-capacitor. Available Online: https://se.mathworks.com/help/physmod/sps/powersys/ref/supercapacitor.html. (accessed on 11 August 2019).